ACS APPLIED MATERIALS & INTERFACES

Research Article

www.acsami.org

Solution-Processable Silicon Phthalocyanines in Electroluminescent and Photovoltaic Devices

Eli Zysman-Colman,*[,†] Sanjay S. Ghosh,[‡,§] Guohua Xie,[‡] Shinto Varghese,[‡] Mithun Chowdhury,[‡] Nidhi Sharma,[†,‡] David B. Cordes,[†] Alexandra M. Z. Slawin,[†] and Ifor D. W. Samuel*[,‡]

[†]Organic Semiconductor Centre, EaStCHEM School of Chemistry, University of St Andrews, St Andrews, Fife, KY16 9ST U.K.

[‡]Organic Semiconductor Centre, SUPA, School of Physics and Astronomy, University of St. Andrews, St. Andrews, Fife, KY16 9SS U.K.

Supporting Information

ABSTRACT: Phthalocyanines and their main group and metal complexes are important classes of organic semiconductor materials but are usually highly insoluble and so frequently need to be processed by vacuum deposition in devices. We report two highly soluble silicon phthalocyanine (SiPc) diester compounds and demonstrate their potential as organic semiconductor materials. Near-infrared (λ_{EL} = 698−709 nm) solution-processed organic light-emitting diodes (OLEDs) were fabricated and exhibited external quantum efficiencies (EQEs) of up to 1.4%. Binary bulk heterojunction solar cells employing P3HT or PTB7 as the donor and the SiPc as the acceptor provided power conversion efficiencies (PCE) of up to 2.7% under simulated solar illumination. Our results show that soluble SiPcs are promising materials for organic electronics.

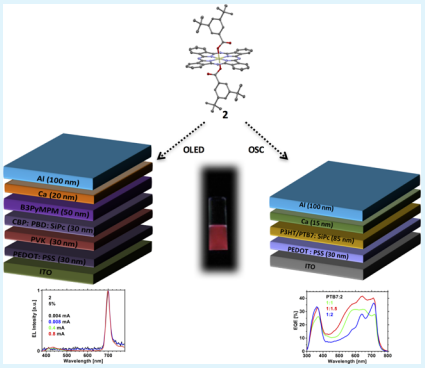

KEYWORDS: *silicon phthalocyanines, single crystals, near-IR emission, solution-processable organic light-emitting diodes, organic solar cells*

INTRODUCTION

Phthalocyanines (Pcs) are thermally and chemically stable planar 18 π-electron aromatic macrocycle analogs of porphyrins consisting of four nitrogen-linked isoindole units. Pcs and their metal complexes have attracted tremendous recent interest in materials science due to their diverse optoelectronic and magnetic properties.[1] Notable in particular is the impressive light-harvesting capacity of Pcs as a result of intense absorption of the Q-bands in the region of 700 nm.[2] Metal complexes of Pcs have thus historically been used as blue-green dyes and pigments.[2] Phthalocyanines have been incorporated into a wide range of functional devices ranging from organic field effect transistors,[3,4] sensors,[3] optical storage devices, organic light-emitting diodes (OLEDs),[5] and organic (OSC) and dye-sensitized solar cells (DSSC).[6−8] Silicon phthalocyanines (SiPcs) are a particularly attractive subclass of Pcs given the elemental abundance and very low toxicity levels of silicon coupled with their low band gap (~1.7 eV). However, to date, only a single report exists on the use of SiPcs as emitters in OLEDs, and there are but a handful of reports of SiPcs used as dyes in solar cells.[6,9−12] The very low solubility in common organic solvents of SiPcs is very likely a contributing factor to the paucity of reports of OLED and solar cell devices. Here, we demonstrate that by disubstituting at the axial positions of SiPc complexes with suitably functionalized carboxylate groups (**1** and **2**, Figure 1a), solubility of these materials in organic solvents can be readily enhanced, and solution-processed NIR OLEDs and OSCs can be fabricated. Solution-processed devices are attractive and exciting alternatives to vacuum-deposited devices as fabrication relies on robust and high-throughput infrastructure to produce large-area devices at significantly reduced cost.[13]

RESULTS AND DISCUSSION

Synthesis and Compound Characterization. SiPc **1** and **2** were prepared in modest yield by the substitution of the axial chloride ligands of commercially available silicon phthalocyanine dichloride, $SiPcCl_2$, with, respectively, eicosanoic acid and 3,5-di-*tert*-butylbenzoic acid in diglyme at 160 °C (Figure 1a). These compounds were easily purified by column chromatography, wherein each of **1** and **2** eluted first as a distinct blue band. The purity and identity of the compounds was confirmed by ^{1}H NMR spectroscopy, high-resolution mass spectrometry, and elemental analysis. The melting point of **1** was found to be 168−170 °C, and that of **2** is significantly higher at >380 °C. Both compounds are highly soluble in chlorinated solvents but insoluble in polar aprotic solvents such as acetonitrile. Solubility of these compounds in chlorinated solvents such as in 1,2-dichlorobenzene [**1** (>10 mg mL^{-1}) and **2** (>35 mg mL^{-1})]

Received: December 18, 2015
Accepted: March 18, 2016
Published: March 18, 2016

DOI: 10.1021/acsami.5b12408
ACS Appl. Mater. Interfaces 2016, 8, 9247−9253

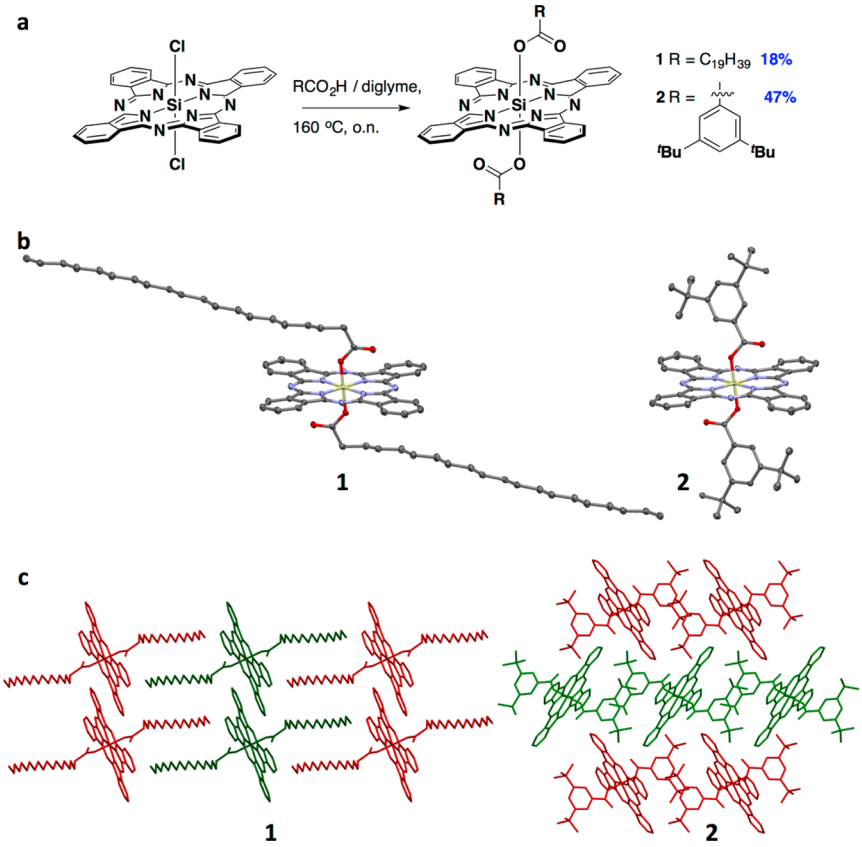

Figure 1. (a) Synthesis of SiPc **1** and **2**. (b) Structures of **1** and **2** (50% probability ellipsoids; H atoms omitted for clarity). Heteroatoms: O, red; N, blue; Si, yellow. Selected bond lengths (Å): (**1**) Si–O 1.7472(9), Si–N_1 1.9065(11), Si–N_2 1.9161(16); (**2**) Si_1–O_1 1.7485(17), Si_{41}–O_1 1.7518(17), Si_1–N_1 1.906(2), Si_1–N_2 1.913(2), Si_{41}–N_1 1.898(2), Si_{41}–N_2 1.9188(19). (c) Solid-state arrangements of **1** and **2**.

Table 1. Optoelectronic Characterization Data for 1 and 2[a]

	λ_{abs} /nm [$\varepsilon/10^4$ M^{-1} cm^{-1}]	λ_{em} /nm	Φ_{PL}/%[b]	τ_e/ns	HOMO/eV	LUMO/eV	ΔE /eV
1	291 [2.4], 360 [7.1], 614 [3.8], 652 [3.2], 683 [26]	690	50	7.0	−5.39	−3.64	1.75
2	291 [2.4], 359 [7.1], 616 [3.7], 654 [3.1], 685 [27]	690	48	7.1	−5.40	−3.66	1.74

[a]Measurements in DCM at 298 K. For electrochemistry, 0.1–0.2 M n-Bu_4NPF_6 was added as the supporting electrolyte to the solution, and Fc/Fc^+ was used as the internal reference; glassy-carbon working electrode, platinum-spiral counter electrode, and platinum-wire quasi-reference electrode were used at a scan rate of 0.1 V s^{-1}. The HOMO and LUMO energies were calculated using the relation $E_{HOMO/LUMO} = -(E^{ox}/E^{red} + 4.8)$ eV, where E^{ox} and E^{red} are first oxidation and reduction potentials, respectively. $\Delta E = -(E_{HOMO} - E_{LUMO})$.[17] [b]Measured in an integrating sphere (see the Supporting Information for details).

make these compounds amenable for solution processing in optoelectronic devices (vide infra).

Additionally, single crystals of suitable quality for X-ray diffraction structure analysis were grown by slow evaporation of mixed solutions of CH_2Cl_2–ethanol for **1** and CH_2Cl_2–acetonitrile for **2**. Their structures are shown in Figure 1b. Each SiPc possesses a hypervalent silicon(IV) in a distorted octahedral SiN_4O_2 coordination environment with a crystallographic inversion center at the silicon atom; therefore, the SiN_4 fragment is planar (irrespective of any distortions within the phthalocyanine ring itself), the SiO_2 fragment is linear, and only two of the Si–N and one of the Si–O bonds are unique. The Si–N bonds are significantly longer [1.9065(11)–1.9188(19) Å] than the Si–O bonds [1.7472(9)–1.7518(17) Å]. The axial carboxylate ligands disrupt intermolecular interaction in the solid state and significantly increase the solubility of these SiPcs. The linear alkyl chains of the eicosanoate ligands present in **1** are arranged parallel to the plane of the phthalocyanine ring, whereas the 3,5-di-*tert*-butylbenzoate ligands in **2** are arranged nearly orthogonal to the Pc plane. As a function of the differences in orientation of the carboxylate ligands, **1** packs with coparallel but diagonally offset Pc rings with Si···Si distances of 9.1436(15) Å, and **2** packs in a herringbone motif with two crystallographically distinct SiPc compounds, resulting in much longer Si···Si distances of 11.313(2) Å. Neither **1** nor **2** show any intermolecular $\pi\cdots\pi$ and C–H···π interactions (Figure 1c).

Optoelectronic Properties. Compounds **1** and **2** exhibit nearly identical electrochemistry in dichloromethane (DCM) solution (Table 1). Reversible oxidation waves were found at 0.59 and 0.60 V for **1** and **2**, respectively, versus Fc/Fc^+. These values are similar to alkoxy-disubstituted SiPcs.[14] SiPc **1** shows a single reversible reduction wave at −1.16 V (a second irreversible reduction wave is present at more negative potentials), while for SiPc **2**, two reversible waves at −1.14 and −1.57 V are observed (cyclic voltammograms shown in Figure S1). These potentials are typical of the redox processes centered on the Pc macrocycle.[15] The reduction wave at −1.57

DOI: 10.1021/acsami.5b12408
ACS Appl. Mater. Interfaces 2016, 8, 9247–9253

V is assigned to a second reduction of the Pc ring system. The first reduction potentials in **1** and **2** are cathodically shifted by ca. 170 mV compared to axially alkoxy-disubstituted SiPcs (E_{red} = −990 mV).[16] The redox gaps for both compounds are similar, ranging from 1.74 to 1.75 V. Both SiPc compounds are intensely blue solids. In DCM solution, their absorption spectra are dominated by sharp Q-band transitions at 683 nm for **1** and 685 nm for **2** ($\varepsilon = 26 \times 10^4$ M^{-1} cm^{-1} for **1** and 27×10^4 M^{-1} cm^{-1} for **2**). There are lower intensity high-energy absorption Soret bands spanning 290−400 nm that are characteristic of silicon phthalocyanines (Table 1).[2]

Both compounds emit strongly in the near-infrared (NIR) in DCM solution with λ_{max} of 691 nm (cf. Figure S2 for **1** and Figure 2 for **2**). They show similar photoluminescence

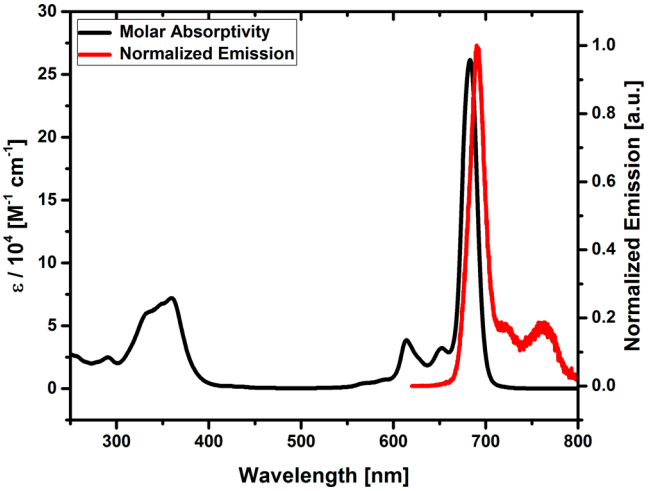

Figure 2. Normalized absorption and emission spectra of **2** in DCM at 298 K.

quantum yields, Φ_{PL}, of 50 and 48% for **1** and **2**, respectively (Table 1). These values are typical of SiPc compounds, although the emission is modestly red-shifted compared to alkoxy- and silyloxy-disubstituted silicon phthalocyanines.[2] The short monoexponentially decaying emission lifetimes (τ_e ca. 7 ns), the mirror image spectral features (cf. Figure 2), and the small Stokes shifts all point to emission originating from the lowest excited singlet state. The emission is significantly quenched in the neat solid (Φ_{PL} < 1%).

Organic Light-Emitting Diodes. The high efficiency and narrow spectral range of luminescence make the SiPc suitable luminophores for NIR light sources. NIR light sources offer distinct advantages for sensing, information security, and imaging, particularly in a biological context where tissue samples exhibit minimal absorption and autofluorescence.[18−21] To the best of our knowledge, there is only one report on the use of SiPc compounds as emitters in OLEDs, and the external quantum efficiency (EQE) was not reported.[14] A further report describes the use of SiPc compounds in electrochemiluminescence studies.[22] The electroluminescence of SiPc **1** and **2** was studied in organic light-emitting diodes (OLED). The device architecture is shown in Figure 3 and consists of the following layers: ITO/PEDOT:PSS (30 nm)/PVK (30 nm)/CBP:PBD:SiPc [30:(70−*x*):*x*; *x* = 1, 5, or 10 wt %; SiPc = **1** or **2**; 30 nm]/B3PYMPM (50 nm)/Ca (20 nm)/Al (100 nm). PEDOT:PSS is a hole-injecting layer. Poly(*N*-vinylcarbazole) (PVK) is a hole-transporting and electron- and exciton-blocking layer with lowest-unoccupied molecular orbital

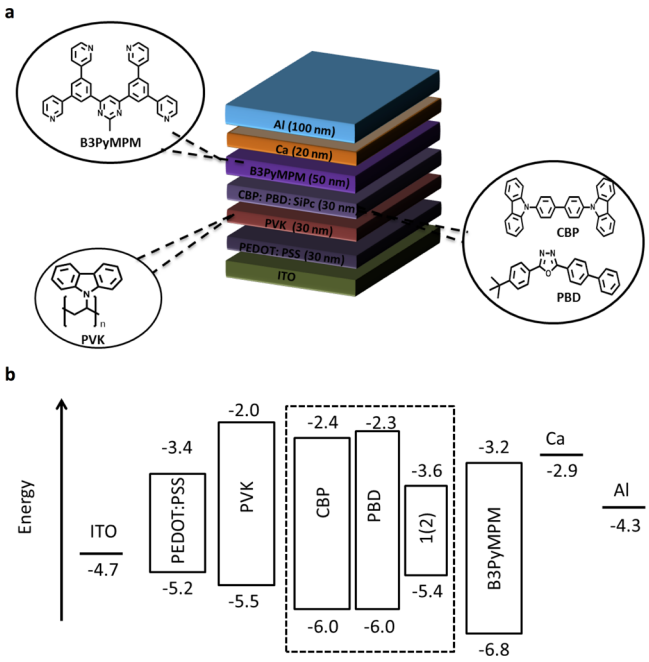

Figure 3. (a) Device configuration of the OLEDs. (b) Energy-level diagram of the OLEDs.

(LUMO) of 2.0 eV.[23,24] *N*,*N*′-Dicarbazolyl-4−4′-biphenyl (CBP) and 2-(4-*tert*-butylphenyl)-5-(4-biphenylyl)-1,3,4-oxadiazole (PBD) are the hosts. These three layers were deposited by spin-coating. 4,6-Bis(3,5-di(pyridin-3-yl)phenyl)-2-methylpyrimidine (B3PYMPM) is an electron-transporting and hole-blocking layer with electron mobility of approximately 10^{-5} cm^2 $(V\ s)^{-1}$ and a highest-occupied molecular orbital (HOMO) of 6.8 eV.[25] The multilayer architecture helps to achieve better electroluminescence performance by balancing the hole and electron injection and by confining the excitons in the emitting layer.

The topographical morphology of the emitting layer ITO/PEDOT:PSS (30 nm)/PVK (30 nm)/CBP:PBD:SiPc [30:(70−*x*):*x*; *x* = 1, 5, or 10 wt %; SiPc = **1** or **2**; 30 nm] was measured by optical and atomic force microscopies (OM and AFM). The film roughness increases at high doping levels of **2**. At 10 wt % of **2**, the film has pinholes and is visually nonuniform. Pinholes induce current leakage, thereby deteriorating the device performance. In contrast, the films with **1** are of better quality and do not have as many pinholes (Figure 4).

The emitting layer was doped with 1, 5, or 10 wt % SiPc. A higher doping or a neat SiPc were not used to avoid concentration quenching of the luminescence. Both **1** and **2** exhibit NIR electroluminescence (EL) in the OLED. Their EL spectra are similar to their photoluminescence spectra (Figure 5). The EL spectra show maxima ranging from 698−709 nm and have full width at half-maximum of 21−27 nm that are especially narrow for a near IR organic emitter.

The current, voltage, and light-output characteristics of the OLED employing **2** as the emitter are shown in Figure 6. Light output of OLEDs is often expressed in photometric units (i.e., units that take account of the responsivity of the eye, such as cd m^{-2}). Because we are interested in NIR emission, the eye response is not relevant, and so instead, we show the power per unit area emitted, a quantity known as radiant exitance. For the 1 wt % sample shown, NIR light output is obtained for applied voltages of 5 V and more. The external quantum efficiency

DOI: 10.1021/acsami.5b12408
ACS Appl. Mater. Interfaces 2016, 8, 9247−9253

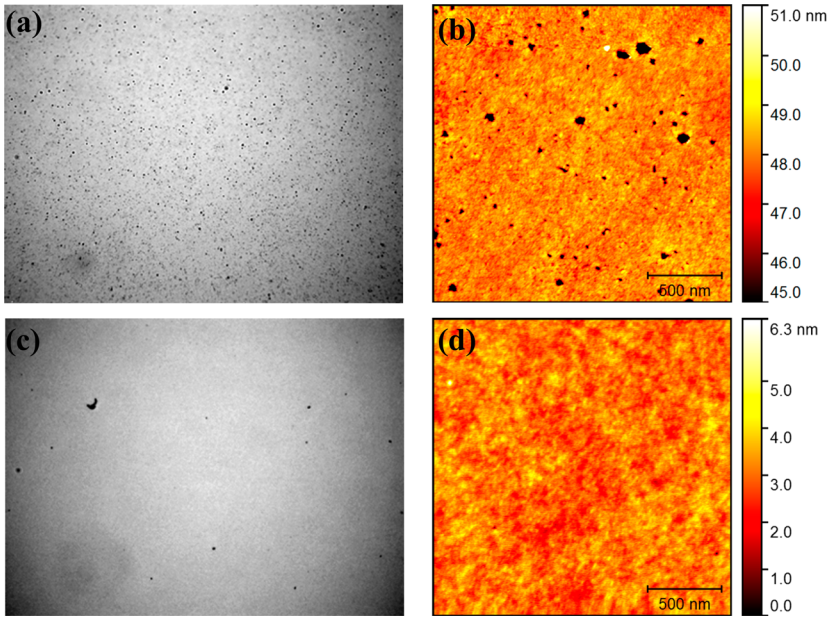

Figure 4. Optical microscopy [(a,c); 150 × 113 μm^2 each] and atomic-force microscopy [(b,d); 2 × 2 μm^2 each; 500 nm scale bar] of films ITO/PEDOT:PSS/PVK/CBP:PBD:SiPc (30:60:10; SiPc = **1** or **2**; 30 nm). The film doped with **2** [(a,b)] has more pinholes and higher RMS roughness Ra = 0.72 nm than the film doped with **1** [(c,d); Ra = 0.4 nm].

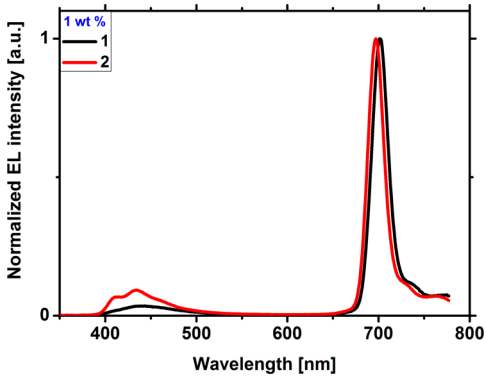

Figure 5. Electroluminescence spectra for **1** and **2**.

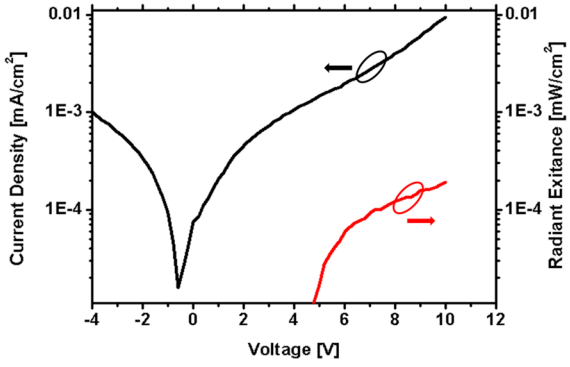

Figure 6. Current density vs voltage (black) and radiant exitance vs voltage (red) for **2**.

(EQE) is up to 1.4%, which ranks among the most efficient solution-processed fluorescent NIR OLEDs.[26−30] Higher current densities and light output are obtained for higher concentrations of **2** (Figure 6), although the overall efficiency is lower, probably because of a combination of concentration quenching of luminescence and deterioration of film quality (Table 2). The EL at high current comes both from **2** in the NIR at >660 nm and from the hosts in the visible range at 380−560 nm, even at high doping levels of **2**.

Table 2. OLED Performance Data

device	SiPc[a]	V_{on}[b] (V)	λ_{EL}(nm)	fwhm/nm	EQE (J_{eqe}) (% (mA/cm²))
1	**1** (1%)	9.9	701	22	0.64 (1.5)
2	**1** (5%)	11.5	704	24	0.45 (0.025)
3	**1** (10%)	8.6	709	27	0.38 (0.07)
4	**2** (1%)	7.4	700	21	1.40 (0.002)
5	**2** (5%)	8.6	700	22	0.41 (0.14)
6	**2** (10%)	6.9	698	22	0.13 (23.3)

[a]Doping concentrations in parentheses. [b]Turn-on voltage that gives an irradiance of 10^{-4} mW cm^{-2}

For **1**, the variation of current density matches that of irradiance (Figure S6. The host EL is negligible, indicating efficient host-to-**1** energy transfer. The maximum irradiance and EQE are achieved at 1 wt % of **1** to give EQE of 0.64%, which is only half that of **2**. In contrast, **1** outperforms **2** at higher doping: the EQE at 5 and 10 wt % of **1** is 0.45 and 0.38%, respectively, while that of **2** is 0.41 and 0.13%. The turn-on voltage for **1**, however, is higher than that for **2** (Table 2). The lower efficiencies in **1** compared to **2** may be the result of the insulating alkyl chains present that may lower charge mobility in the film.

Organic Solar Cells. Silicon phthalocyanines have been explored more widely as dyes and electron donors and acceptors in photovoltaic applications than in EL devices. The highest power conversion efficiency (PCE) in a dye-sensitized solar cell (DSSC) employing an SiPc dye with the adsorbing carboxylate unit directly attached to the Pc macrocycle was recently reported by Sellinger and co-workers to be 4.5%, with a short-circuit current of 19.0 mA cm^{-2}.[6] PCEs decrease markedly when the adsorbing unit is attached to the axial ligands about the SiPc.[31,32] Silicon phthalocyanines

DOI: 10.1021/acsami.5b12408
ACS Appl. Mater. Interfaces 2016, 8, 9247−9253

bearing tri-*n*-hexylsilyloxy axial substituents have been used as additives in ternary bulk heterojunction (BHJ) organic solar cells (OSC), where they act not only as dyes but also as charge transporting agents.[33−35] Efficiencies for these devices reach up to 4.9%.[35] The replacement of *n*-hexylsiyloxy groups with fluorinated phenoxy moieties resulted in improved PCE (>2%) in planar heterojunction OSCs, where the SiPcs can act as both electron donors or electron acceptors.[34]

In BHJ solar cells, fullerene derivatives are widely used as acceptors, but their weak absorption in the visible spectrum, the difficulty in tuning the band gap by chemical modification, and their high price are all detracting features, which has catalyzed the search for replacement candidate non-fullerene acceptor (NFA) materials.[36] Among NFA materials investigated to date, those based on perylenediimide (PDI) have been widely explored as they possess electron affinities, EA, around 3.9 eV, which are similar to fullerene acceptors.[37] Recently, a PCE of 7.16% has been reported using a wide-band gap polymer PDBT-T1 donor in concert with a perylene bisimide dimer as an acceptor in BHJ organic solar cells.[38] Cnops and co-workers reported a PCE of 6.8% using boron subphthalocyanine (BsubPc)-based donor and acceptor materials.[39] Indeed, PCEs for state-of-the-art NFA OSC have exceeded 8% for evaporated three-layer devices based on BsubPc acceptors[40] while PCEs of 6.8% have been obtained for solution-processed planar heterojunction photovoltaic devices using a bespoke conjugated acceptor.[41] Acceptors based on phthalocynanines have also been explored, and the handful of reports in literature in which silicon and germanium phthalocyanines are used as acceptors in planar heterojunction photovoltaic devices show PCEs in the devices of only up to 2%.[10,11,34]

SiPcs and **1** and **2** were investigated as dyes and electron-acceptor materials in binary BHJ OSCs in conjunction with electron donor polymers P3HT or PTB7 (Figure 7). A reference device based on PTB7:PC71BM was fabricated and showed a PCE of 6.4% (Figure S9). In the reference device, 1,8-diiodooctane (DIO) was used as an additive to improve the morphology of the blends. The obtained PCE is in close agreement with the values reported in the literature.[42,43] The current density−voltage (J−V) characteristics of the OSCs using SiPc acceptors are shown in Figure 8, and the device data

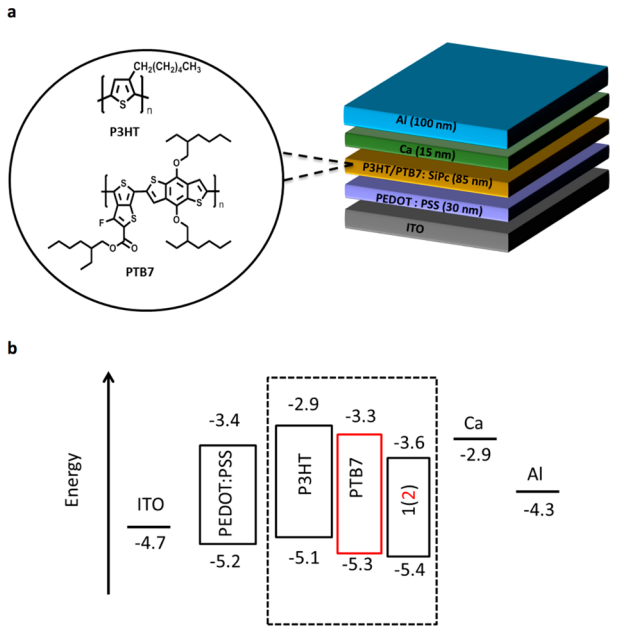

Figure 7. (a) Device configuration of the OSCs. (b) Energy level diagram of the OSCs.

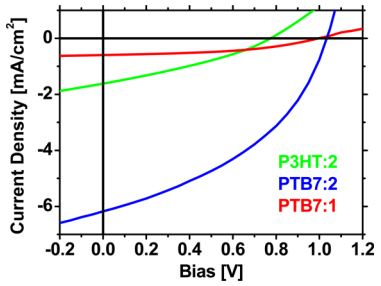

Figure 8. Current−voltage characteristics of OSCs under AM1.5G illumination.

Table 3. Optimized OSC Performance Data[a]

OSC	ratio	T_{anneal} (°C)	J_{SC} (mA cm^{-2})	V_{OC} (V)	FF (%)	PCE (%)
PTB7:**1**	1:1.5	100	0.60	1.00	45	0.27
PTB7:**2**	1:1.5	100	6.18	1.03	42	2.67
P3HT:**2**	1:1	120	1.62	0.77	32	0.40

[a]Under 100 mW cm^{-2} AM1.5G illumination. Annealed for 10 min.

is summarized in Table 3. The V_{OC} of the OSC employing P3HT as the donor is 0.26 V less than when PTB7 acts as the donor. This difference can be attributed to the HOMO of P3HT (−5.1 eV) being destabilized compared to PTB7 (−5.31 eV) by a similar value. The higher V_{OC} of the PTB7:**2** OSC combined with the significantly enhanced J_{SC} of 6.18 mA cm^{-2} results in a far more efficient device (PCE = 2.67%). This PCE, although lower than the reference OSC, is nevertheless superior to the previous OSCs using SiPc or GePc acceptor materials. Replacement of **2** with **1** as the acceptor results in an order of magnitude lower short-circuit current (J_{SC} = 0.60 mA), which we speculate is due to the reduced charge mobility of the SiPc dye due to the insulating eicosanoate groups. A disadvantage of PC60BM, which is widely used as an acceptor, is its weak absorption. It is desirable for acceptors to contribute to light absorption. We investigated this by measuring the EQE spectra for a range of donor/acceptor weight ratios, and the results for PTB7:**2** and P3HT:**2** are shown in Figure 9 and in Figure S8, respectively. The peak in the region of 360 nm is due to absorption of **2**. In addition it can be seen that **2** contributes to

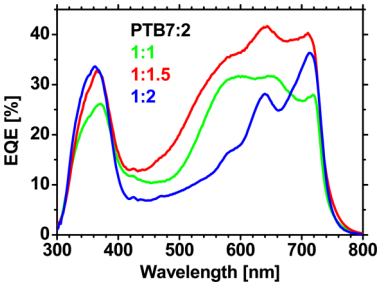

Figure 9. External quantum efficiency spectra of OSCs at various PTB7:**2** ratios.

DOI: 10.1021/acsami.5b12408
ACS Appl. Mater. Interfaces 2016, 8, 9247−9253

the absorption in the region of 720 nm. Hence our results show that the absorption of **2** contributes to the photocurrent. The highest efficiency is for a 1:1.5 weight ratio of PTB7:**2** and suggest this blend ratio gives the best combination of absorption and electron transport. AFM studies on PTB7:**2** films for the weight ratio 1:1.5 (Figure S7) demonstrate that annealing at 100 °C leads to the pure phase formation of each component, which in turn increases the carrier mobility and enhances the device performance. The 1:1 blend is most likely less efficient due to worse electron transport, and the 1:2 blend is likely to have better electron transport but lower absorption.

The annealing temperature of the active layer is another key parameter in the construction of the optimized OSC.[44] Table 4 shows relative OSC performance metrics as a function of annealing temperature. An annealing temperature (T_{anneal}) of 100 °C produced a device with the best combination of short-circuit current and fill factor values. Increasing the annealing temperature beyond 120 °C resulted in a significant decrease in both J_{SC} and FF, and annealing temperatures inferior to 100 °C produced a suboptimal short-circuit current. The poorest performing device was the one where there was no thermal annealing with J_{SC} and FF values of 3.10 mA/cm^2 and 26%, respectively.

Table 4. OSC Performance Data Employing PTB7:2.[a]

T_{anneal} (°C)	PCE (%)	J_{SC} (mA cm^{-2})	V_{OC} (V)	FF (%)
none	0.80	3.10	0.99	26
80	2.33	5.59	1.02	41
100	2.67	6.18	1.03	42
120	2.60	6.27	1.04	40
140	1.95	5.52	1.04	34
160	1.13	3.75	1.04	29

[a]Under 100 mW cm^{-2} illumination. At 1:1.5 PTB7:**2** weight ratio annealed for 10 min.

CONCLUSIONS

We demonstrated that with appropriate axial disubstitution, high solubility in chlorinated solvents can be conferred to SiPc carboxylate compounds. Silicon phthalocyanines act as both efficient near-IR emitters and strong light-absorbers. Their electrochemical properties make them suitable as electron-accepting materials in OSCs. SiPc **2** exhibited the greatest potential, with the OLED showing the highest external quantum efficiency of 1.4% and the OSC the highest power conversion efficiency of 2.67%. The abundance and negligible toxicity profile of silicon makes it an attractive element to be incorporated into functional materials. These promising results augur well for future developments in silicon-based organic electronics.

ASSOCIATED CONTENT

Supporting Information

The Supporting Information is available free of charge on the ACS Publications website at DOI: 10.1021/acsami.5b12408.

Additional details on synthesis, X-ray crystallography, electrochemistry, absorption and emission spectroscopy, organic light-emitting diodes, organic solar cells, and NMR spectra. A table showing crystal data and structure refinement. Figures showing cyclic voltammograms of **1** and **2**, absorption and emission spectra of **1** in dichloromethane, AFM images of films, electroluminescence spectra of OLED, OLED analysis, additional AFM images, EQE curve for **P3HT**, current−voltage characteristics, absorption spectra of films, and NMR spectra. (PDF)

The research data supporting this publication can be accessed at http://dx.doi.org/10.17630/129a22c4-55bd-402b-af9f-2fe87d09fbd0.

CIF of the crystal structures for **1** and **2**, CCDC nos. 1434986 and 1434992 (CIF)

AUTHOR INFORMATION

Corresponding Authors

*Tel: +44-1334 463826; fax: +44-1334 463808; e-mail: eli.zysman-colman@st-andrews.ac.uk.

*E-mail: idws@st-andrews.ac.uk.

Present Address

[§]Optoelectronics Laboratory, Department of Physics, North Maharashtra University, Jalgaon-425001, India

Notes

The authors declare no competing financial interest.

ACKNOWLEDGMENTS

E..Z.-C. acknowledges the University of St. Andrews for financial support. We thank the EPSRC UK National Mass Spectrometry Facility at Swansea University for analytical services. I.D.W.S. acknowledges support from the EPSRC (grant EP/J01771X), the European Research Council (grant 321305), and a Royal Society Wolfson Research Merit Award. We thank Dr. Nail Shavaleev for the synthesis of **1** and **2**, for electrochemical measurements, for contributions to the UV−vis spectroscopy measurements and for suggesting the choice of materials.

REFERENCES

(1) de la Torre, G.; Claessens, C. G.; Torres, T. S. Phthalocyanines: Old Dyes, New Materials. Putting color in Nanotechnology. *Chem. Commun.* **2007**, 2000−2015.

(2) Nyokong, T. Effects of Substituents on the Photochemical and Photophysical Properties of Main Group Metal Phthalocyanines. *Coord. Chem. Rev.* **2007**, *251*, 1707−1722.

(3) Guillaud, G.; Simon, J.; Germain, J. P. Metallophthalocyanines: Gas Sensors, Resistors and Field Effect Transistors1. *Coord. Chem. Rev.* **1998**, *178*−*180* (2), 1433−1484.

(4) Melville, O. A.; Lessard, B. H.; Bender, T. P. Phthalocyanine-Based Organic Thin-Film Transistors: A Review of Recent Advances. *ACS Appl. Mater. Interfaces* **2015**, *7*, 13105−18.

(5) Hohnholz, D.; Steinbrecher, S.; Hanack, M. Applications of Phthalocyanines in Organic Light Emitting Devices☆. *J. Mol. Struct.* **2000**, *521*, 231−237.

(6) Lim, B.; Margulis, G. Y.; Yum, J.-H.; Unger, E. L.; Hardin, B. E.; Grätzel, M.; McGehee, M. D.; Sellinger, A. Silicon-Naphthalo/Phthalocyanine-Hybrid Sensitizer for Efficient Red Response in Dye-Sensitized Solar Cells. *Org. Lett.* **2013**, *15*, 784−787.

(7) Martin-Gomis, L.; Fernandez-Lazaro, F.; Sastre-Santos, A. Advances in Phthalocyanine-Sensitized Solar Cells (PcSSCs). *J. Mater. Chem. A* **2014**, *2*, 15672−15682.

(8) Ragoussi, M.-E.; Ince, M.; Torres, T. Recent Advances in Phthalocyanine-Based Sensitizers for Dye-Sensitized Solar Cells. *Eur. J. Org. Chem.* **2013**, *2013*, 6475−6489.

(9) Honda, S.; Ohkita, H.; Benten, H.; Ito, S. Selective Dye Loading at the Heterojunction in Polymer/Fullerene Solar Cells. *Adv. Energy Mater.* **2011**, *1*, 588−598.

DOI: 10.1021/acsami.5b12408
ACS Appl. Mater. Interfaces 2016, 8, 9247−9253

(10) Lessard, B. H.; Grant, T. M.; White, R.; Thibau, E.; Lu, Z.-H.; Bender, T. P. The Position and Frequency of Fluorine Atoms Changes the Electron Donor/Acceptor Properties of Fluorophenoxy Silicon Phthalocyanines Within Organic Photovoltaic Devices. *J. Mater. Chem. A* **2015**, *3*, 24512−24524.
(11) Lessard, B. H.; White, R. T.; Al-Amar, M.; Plint, T.; Castrucci, J. S.; Josey, D. S.; Lu, Z.-H.; Bender, T. P. Assessing the Potential Roles of Silicon and Germanium Phthalocyanines in Planar Heterojunction Organic Photovoltaic Devices and How Pentafluoro Phenoxylation Can Enhance $\pi-\pi$ Interactions and Device Performance. *ACS Appl. Mater. Interfaces* **2015**, *7*, 5076−5088.
(12) Xu, H.; Ohkita, H.; Tamai, Y.; Benten, H.; Ito, S. Interface Engineering for Ternary Blend Polymer Solar Cells with a Heterostructured Near-IR Dye. *Adv. Mater.* **2015**, *27*, 5868−5874.
(13) Duggal, A. R.; Heller, C. M.; Shiang, J. J.; Liu, J.; Lewis, L. N. Solution-Processed Organic Light-Emitting Diodes for Lighting. *J. Disp. Technol.* **2007**, *3*, 184−192.
(14) Flora, W. H.; Hall, H. K.; Armstrong, N. R. Guest Emission Processes in Doped Organic Light-Emitting Diodes: Use of Phthalocyanine and Naphthalocyanine Near-IR Dopants. *J. Phys. Chem. B* **2003**, *107*, 1142−1150.
(15) Xu, H.; Wada, T.; Ohkita, H.; Benten, H.; Ito, S. Dye Sensitization of Polymer/Fullerene Solar Cells Incorporating Bulky Phthalocyanines. *Electrochim. Acta* **2013**, *100*, 214−219.
(16) Lever, A. B. P.; Minor, P. C. Electrochemistry of Main-Group Phthalocyanines. *Inorg. Chem.* **1981**, *20*, 4015−4017.
(17) Cardona, C. M.; Li, W.; Kaifer, A. E.; Stockdale, D.; Bazan, G. C. Electrochemical Considerations for Determining Absolute Frontier Orbital Energy Levels of Conjugated Polymers for Solar Cell Applications. *Adv. Mater.* **2011**, *23*, 2367−2371.
(18) Xiang, H.; Cheng, J.; Ma, X.; Zhou, X.; Chruma, J. J. Near-infrared Phosphorescence: Materials and Applications. *Chem. Soc. Rev.* **2013**, *42*, 6128−6185.
(19) Qian, G.; Wang, Z. Y. Near-Infrared Organic Compounds and Emerging Applications. *Chem. - Asian J.* **2010**, *5*, 1006−1029.
(20) Peng, X.; Draney, D. R.; Volcheck, W. M.; Bashford, G. R.; Lamb, D. T.; Grone, D. L.; Zhang, Y.; Johnson, C. M. *Phthalocyanine Dye as an Extremely Photostable and Highly Fluorescent Near-Infrared Labeling Reagent*. *Proc. SPIE* **2006**, 60970E-60970E−12.
(21) Pansare, V. J.; Hejazi, S.; Faenza, W. J.; Prud'homme, R. K. Review of Long-Wavelength Optical and NIR Imaging Materials: Contrast Agents, Fluorophores, and Multifunctional Nano Carriers. *Chem. Mater.* **2012**, *24*, 812−827.
(22) Wheeler, B. L.; Nagasubramanian, G.; Bard, A. J.; Schechtman, L. A.; Kenney, M. E. A Silicon Phthalocyanine and a Silicon Naphthalocyanine: Ssynthesis, Electrochemistry, and Electrogenerated Chemiluminescence. *J. Am. Chem. Soc.* **1984**, *106*, 7404−7410.
(23) Zhang, S.; Turnbull, G. A.; Samuel, I. D. W. Highly Efficient Solution-Processable Europium-Complex Based Organic Light-Emitting Diodes. *Org. Electron.* **2012**, *13*, 3091−3096.
(24) Kido, J.; Hongawa, K.; Okuyama, K.; Nagai, K. Bright Blue Electroluminescence from Poly(N-vinylcarbazole). *Appl. Phys. Lett.* **1993**, *63*, 2627−2629.
(25) Sasabe, H.; Kido, J. Multifunctional Materials in High-Performance OLEDs: Challenges for Solid-State Lighting†. *Chem. Mater.* **2011**, *23*, 621−630.
(26) Borek, C.; Hanson, K.; Djurovich, P. I.; Thompson, M. E.; Aznavour, K.; Bau, R.; Sun, Y.; Forrest, S. R.; Brooks, J.; Michalski, L.; Brown, J. Highly Efficient, Near-Infrared Electrophosphorescence from a Pt−Metalloporphyrin Complex. *Angew. Chem., Int. Ed.* **2007**, *46*, 1109−1112.
(27) Yang, Y.; Farley, R. T.; Steckler, T. T.; Eom, S.-H.; Reynolds, J. R.; Schanze, K. S.; Xue, J. Efficient Near-Infrared Organic Light-Emitting Devices Based on Low-Gap Fluorescent Oligomers. *J. Appl. Phys.* **2009**, *106*, 044509.
(28) Qian, G.; Zhong, Z.; Luo, M.; Yu, D.; Zhang, Z.; Wang, Z. Y.; Ma, D. Simple and Efficient Near-Infrared Organic Chromophores for Light-Emitting Diodes with Single Electroluminescent Emission above 1000 nm. *Adv. Mater.* **2009**, *21*, 111−116.
(29) Yao, L.; Zhang, S.; Wang, R.; Li, W.; Shen, F.; Yang, B.; Ma, Y. Highly Efficient Near-Infrared Organic Light-Emitting Diode Based on a Butterfly-Shaped Donor−Acceptor Chromophore with Strong Solid-State Fluorescence and a Large Proportion of Radiative Excitons. *Angew. Chem., Int. Ed.* **2014**, *53*, 2119−2123.
(30) The EQE of 1.4% corresponds to that uniquely arising from the guest.
(31) Lin, K. C.; Wang, L.; Doane, T.; Kovalsky, A.; Pejic, S.; Burda, C. Combination of Optical and Electrical Loss Analyses for a Si-Phthalocyanine Dye-Sensitized Solar Cell. *J. Phys. Chem. B* **2014**, *118*, 14027−36.
(32) Liu, J.; Yang, X.; Sun, L. Axial Anchoring Designed Silicon-Porphyrin Sensitizers for Efficient Dye-Sensitized Solar Cells. *Chem. Commun.* **2013**, *49*, 11785−7.
(33) Honda, S.; Nogami, T.; Ohkita, H.; Benten, H.; Ito, S. Improvement of the Light-Harvesting Efficiency in Polymer/Fullerene Bulk Heterojunction Solar Cells by Interfacial Dye Modification. *ACS Appl. Mater. Interfaces* **2009**, *1*, 804−10.
(34) Lessard, B. H.; Dang, J. D.; Grant, T. M.; Gao, D.; Seferos, D. S.; Bender, T. P. Bis(tri-n-hexylsilyl oxide) Silicon Phthalocyanine: A Unique Additive in Ternary Bulk Heterojunction Organic Photovoltaic Devices. *ACS Appl. Mater. Interfaces* **2014**, *6*, 15040−51.
(35) Lim, B.; Bloking, J. T.; Ponec, A.; McGehee, M. D.; Sellinger, A. Ternary Bulk Heterojunction Solar Cells: Addition of Soluble NIR Dyes for Photocurrent Generation Beyond 800 nm. *ACS Appl. Mater. Interfaces* **2014**, *6*, 6905−13.
(36) Nielsen, C. B.; Holliday, S.; Chen, H. Y.; Cryer, S. J.; McCulloch, I. Non-Fullerene Electron Acceptors for Use in Organic Solar Cells. *Acc. Chem. Res.* **2015**, *48* (11), 2803−12.
(37) Li, C.; Wonneberger, H. Perylene Imides for Organic Photovoltaics: Yesterday, Today, and Tomorrow. *Adv. Mater.* **2012**, *24*, 613−36.
(38) Sun, D.; Meng, D.; Cai, Y.; Fan, B.; Li, Y.; Jiang, W.; Huo, L.; Sun, Y.; Wang, Z. Non-Fullerene-Acceptor-Based Bulk-Heterojunction Organic Solar Cells with Efficiency over 7. *J. Am. Chem. Soc.* **2015**, *137*, 11156−62.
(39) Cnops, K.; Zango, G.; Genoe, J.; Heremans, P.; Martinez-Diaz, M. V.; Torres, T.; Cheyns, D. Energy Level Tuning of Non-Fullerene Acceptors in Organic Solar Cells. *J. Am. Chem. Soc.* **2015**, *137*, 8991−7.
(40) Cnops, K.; Rand, B. P.; Cheyns, D.; Verreet, B.; Empl, M. A.; Heremans, P. 8.4% Efficient Fullerene-Free Organic Solar Cells Exploiting Long-Range Exciton Energy Transfer. *Nat. Commun.* **2014**, *5*, 3406.
(41) Lin, Y.; Wang, J.; Zhang, Z.-G.; Bai, H.; Li, Y.; Zhu, D.; Zhan, X. An Electron Acceptor Challenging Fullerenes for Efficient Polymer Solar Cells. *Adv. Mater.* **2015**, *27*, 1170−1174.
(42) Ebenhoch, B.; Thomson, S. A. J.; Genevičius, K.; Juška, G.; Samuel, I. D. W. Charge Carrier Mobility of the Organic Photovoltaic Materials PTB7 and PC71BM and its Influence on Device Performance. *Org. Electron.* **2015**, *22*, 62−68.
(43) Liu, Z.; Ouyang, X.; Peng, R.; Bai, Y.; Mi, D.; Jiang, W.; Facchetti, A.; Ge, Z. Efficient Polymer Solar Cells Sased on the Synergy Effect of a Novel Non-Conjugated Small-Molecule Electrolyte and Polar Solvent. *J. Mater. Chem. A* **2016**, *4*, 2530−2536.
(44) Ito, S.; Hirata, T.; Mori, D.; Benten, H.; Lee, L.-T.; Ohkita, H. Development of Polymer Blend Solar Cells Composed of Conjugated Donor and Acceptor Polymers. *J. Photopolym. Sci. Technol.* **2013**, *26*, 175−180.

DOI: 10.1021/acsami.5b12408
ACS Appl. Mater. Interfaces 2016, 8, 9247−9253